

Phenomenological Theory of the Supercurrent Diode Effect: The Lifshitz Invariant

Denis Kochan^{1,2,*}, Andreas Costa², Iaroslav Zhumagulov², and Igor Žutić³

¹*Institute of Physics, Slovak Academy of Sciences, 84511 Bratislava, Slovakia*

²*Institut für Theoretische Physik, Universität Regensburg, 93053 Regensburg, Germany*

³*University at Buffalo, State University of New York, Buffalo, New York 14260-1500, USA*

(Dated: March 22, 2023)

Nonreciprocal phenomena in the normal state are well established and key to many commercial applications. In contrast, superconducting analogs, such as the superconducting diode effect (SDE), are only starting to be experimentally explored and pose significant challenges to their theoretical understanding. In this work we put forth a phenomenological picture of the SDE based on the generalized Ginzburg-Landau free energy, which includes a Lifshitz invariant as the hallmark of noncentrosymmetric helical phase of the finite-momentum Cooper pairs. We reveal that such a Lifshitz invariant drives the SDE in quasi-two-dimensional systems in an applied magnetic field and cannot be removed by a gauge transformation, due to the inherently inhomogeneous magnetic response. For a thin film, the SDE scales with the square of its thickness and nonlinearly with the strength of the in-plane magnetic field. We derive an explicit formula that relates the SDE at small magnetic fields to the strength of Rashba spin-orbit coupling, g-factor, and Fermi energy. For a noncentrosymmetric Josephson junction, we self-consistently obtain generalized anharmonic current-phase relation which support the SDE. The transparency of our approach, which agrees well with experimentally-measured SDE, offers an important method to study nonreciprocal phenomena, central to superconducting spintronics and topological superconductivity.

Keywords: Lifshitz invariant, supercurrent diode effect, anomalous phase shift, finite-momentum Cooper pairs, noncentrosymmetric Josephson junctions

Introduction: Nonreciprocal response is ubiquitous to many phenomena in classical and quantum physics [1–3]. Faraday and Kerr effects were already well known in the nineteenth century [4, 5], while the nonreciprocity of the semiconducting diodes has enabled many applications in opto-electronics and spintronics [6–9]. However, until the last few years, experimental demonstrations of the nonreciprocal phenomena were largely absent from superconductivity [10, 11].

Recent reports of the superconducting diode effect (SDE) in noncentrosymmetric superconductors and Josephson junctions (JJs) [12–18], have generated a great interest to examine its relevance to other phenomena and their applications [19, 20], as well as to identify an even earlier SDE observations [20, 21]. SDE has nonreciprocal response with the current direction and is often associated with magnetochiral anisotropy [12–18], depending on the vector product of the supercurrent and the applied or proximity-induced magnetic field [22].

With a growing number of materials platforms that supports SDE [12–18, 23–27], there is a continued theoretical debate of its underlying theoretical origin. A common scenario invokes simultaneous breaking of space-inversion, accompanied by the spin-orbit coupling (SOC), and time-reversal symmetries [13, 17, 18, 24, 28–41]. However, there are interesting alternatives suggesting that the nonreciprocal supercurrent originates from inhomogeneous edge transport and stray fields, or from purely orbital effects involving diamagnetic currents, or limitations from asymmetric vortex-protrusions, all without a

need for SOC and Zeeman-related phenomena [42–45].

In this work we present a unified origin of the SDE in different platforms by generalizing phenomenological Ginzburg-Landau (GL) theory [28, 29, 32, 41, 46–50]. With the self-consistent solution of the noncentrosymmetric quasi-two-dimensional (2D) superconductors and superconductor/normal region/ superconductor (S/N/S) JJs, we obtain an excellent agreement with the observed SDE and current-phase relation (CPR) [12, 13, 15, 17, 24, 26]. We further predict overlooked trends for the SDE magnitude with the sample geometry.

Starting from the microscopic Bogoliubov–de Gennes equations in the presence of (i) isotropic Rashba SOC of strength α_R , with the SOC-defined unit vector normal to the film, $\hat{\mathbf{n}}$, and (ii) the magnetic field \mathbf{B} , which yields an orbital coupling and Zeeman interaction, defined by g-factor, g , one systematically derives the generalized GL free-energy density for the condensate wave function ψ [28, 29, 32, 46–49]

$$F = a|\psi|^2 + \frac{b}{2}|\psi|^4 + \frac{|\mathbf{D}\psi|^2}{4m} + \frac{\mathbf{B}^2}{2\mu_0} - \frac{\mathcal{K}}{2}(\hat{\mathbf{n}} \times \mathbf{B}) \cdot \mathbf{Y}_\psi. \quad (1)$$

The first four standard terms are parameterized by coefficients a , b , effective mass m , and the covariant derivative $\mathbf{D} = -i\hbar\nabla - 2e\mathbf{A}$, with the electron charge $e < 0$, and vector potential \mathbf{A} . The last term, $\propto \mathbf{Y}_\psi = (\psi)^*\mathbf{D}\psi + \psi(\mathbf{D}\psi)^*$, is the (isotropic) *Lifshitz invariant* (LI) [51, 52], a figure of merit of the noncentrosymmetry. LI is responsible for the spatial modulation of the order parameter $\psi = e^{i\mathbf{k}_\mathcal{K} \cdot \mathbf{r}}|\psi|$, the helical phase, where the wave vector, $\mathbf{k}_\mathcal{K} \propto 2m\mathcal{K}(\hat{\mathbf{n}} \times \mathbf{B})/\hbar$, with the coupling constant $\mathcal{K} \simeq 3g\mu_B\alpha_R/(\hbar E_F)$ [29][53], of the dimension $\text{m} \cdot \text{C}/\text{kg}$, where E_F is the Fermi energy. We use common coher-

* Corresponding author: denis.kochan@savba.sk

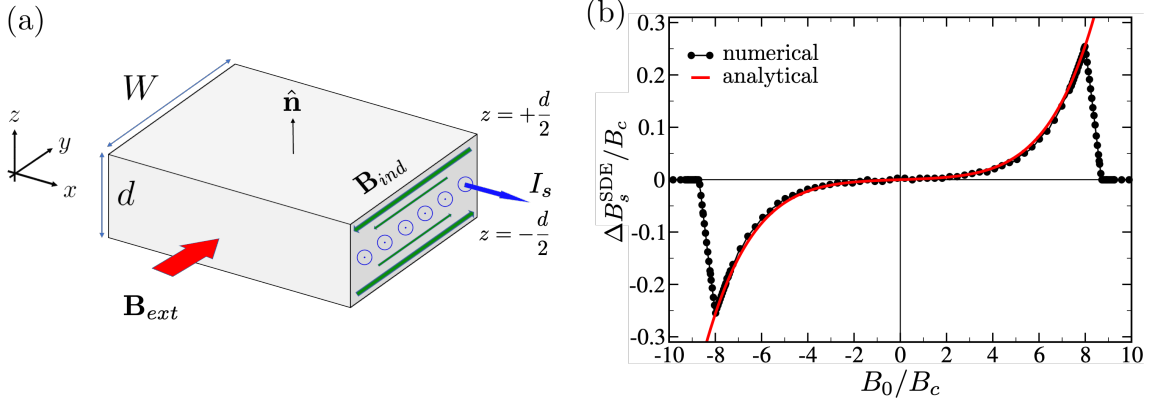


FIG. 1. (a) Schematic of a noncentrosymmetric superconducting film of thickness d , in a constant external in-plane magnetic field, $\mathbf{B}_{ext} = B_0 \hat{y}$, carrying a steady DC supercurrent, I_s , which generates an induced magnetic field, $\mathbf{B}_{ind}(z)$, inside the slab (green arrows). (b) SDE versus in-plane field, B_0 , (in units of the thermodynamic field B_c), for a quasi-2D film. Black symbols: the full numerical solution of Eqs. (5)–(7). Red curve: the analytical result given by Eq. (8) valid in the limit $(d/\lambda)^2 \ll 1$, $(d/\ell)^2 \ll 1$, and $B_I/B_c \ll 1$, with ℓ from Eq. (2). The SDE supercurrent density Δj_s^{SDE} is converted to the corresponding SDE field difference, $\Delta B_s^{\text{SDE}} = \mu_0 \Delta j_s^{\text{SDE}} d/2$, normalized to B_c . For calculations we used: $\xi/\lambda = 1.3$, $\ell/\lambda = 3$, and $d/\lambda = 0.5$.

ence and penetration lengths, ξ , λ , and the thermodynamical critical field, $B_c = \Phi_0/(2\sqrt{2}\pi\lambda\xi)$, where Φ_0 is the magnetic flux quantum. The presence of LI yields an additional scale, the *Lifshitz-Edelstein length* [41]

$$\ell = b/(2\mathcal{K}\mu_0|e||a|). \quad (2)$$

We will use ξ , λ , ℓ , and B_c to express our final results.

After introducing the *shifted momentum operator* $\mathbf{D}_{\mathcal{K}} = \mathbf{D} - \hbar\mathbf{k}_{\mathcal{K}}$, and the *shifted a-coefficient*, $a_{\mathcal{K}} = a - (\hbar\mathbf{k}_{\mathcal{K}})^2/(4m)$, by subtracting, correspondingly, the center-of-mass momentum and energy of the helical Cooper pairs, we obtain the GL equations [54]

$$0 = \frac{\mathbf{D}_{\mathcal{K}}^2}{4m}\psi + a_{\mathcal{K}}\psi + b|\psi|^2\psi, \quad \mathbf{j}_s = \nabla \times \mathbf{H}, \quad (3)$$

where, $\mathbf{H} = \mathbf{B}/\mu_0 + \frac{1}{2}\mathcal{K}(\hat{\mathbf{n}} \times \mathbf{Y}_{\psi})$, and the supercurrent density is

$$\mathbf{j}_s = \frac{e}{2m}\mathbf{Y}_{\psi} - 2e\mathcal{K}|\psi|^2(\hat{\mathbf{n}} \times \mathbf{B}). \quad (4)$$

SDE in thin noncentrosymmetric films: We first consider a quasi-2D film, long and wide (W) compared to ξ , with $\hat{\mathbf{n}} = \hat{z}$, as shown in Fig. 1(a). We assume the film thickness $d \lesssim \xi$, implying that ψ is approximately z -independent. The quasi-2D film is in the constant external (laboratory) in-plane field, $\mathbf{B}_{ext} = B_0 \hat{y}$, and is driven by a steady supercurrent, I_s , with the corresponding density, $I_s/(Wd)$. As a consequence of the supercurrent drive, inside the film, $z \in [-d/2, +d/2]$, there is an induced field, $\mathbf{B}_{ind}(z)$. Therefore, the total resulting field inside the slab, $\mathbf{B} = \mathbf{B}_{ext} + \mathbf{B}_{ind}(z)$, is spatially inhomogeneous, and the LI cannot be removed by a gauge transformation from the quasi-2D free-energy F . This is in contrast to a spatially-homogeneous field treated in Refs. [50, 55]. Such a subtle point is sometimes

overlooked and the removal of the LI by a gauge transformation is erroneously used beyond its applicability.

Given the above assumptions, we look for ψ and \mathbf{B}_{ind} , inside the film, in the forms: $\psi(x) = e^{ikx} f\sqrt{|a|/b}$ and $\mathbf{B}_{ind}(z) = (-2B_I z/d)\hat{y}$, where the unknown real factors, the helical wave vector, k , the dimensionless wave function, $f > 0$, and the induced magnetic field, B_I , will be determined later. Within the Coulomb gauge, the corresponding $\mathbf{A} = A(z)\hat{x} = (B_0 z - B_I z^2/d)\hat{x}$, satisfies $\nabla \times \mathbf{A} = \mathbf{B}_{ext} + \mathbf{B}_{ind}(z)$. By substituting the above $\psi(x)$ and $\mathbf{B}_{ind}(z)$ into the corresponding GL Eq. (3), and $\mathbf{j}_s = j_s(z)\hat{x}$, Eq. (4), one obtains a nonlinear system of differential equations (not explicitly shown here for brevity), which couples k , f , and B_I with $A(z)$, $A^2(z)$ (diamagnetic terms), and their various z -derivatives.

In superconducting thin films [56], the homogeneity of ψ along the z -direction allows one to average the underlying system of differential equations over the thickness. We replace $j_s(z)$, and $A(z)$, and its various powers and z -derivatives, by their averaged values $\langle j_s \rangle = I_s/(Wd)$, $\langle A \rangle = -B_I d/12$, etc., where $\langle O \rangle \equiv \int_{-d/2}^{+d/2} dz O(z)/d$. This averaging removes \mathbf{A} -dependent terms and converts the system of differential equations into an algebraic one

$$k = -\frac{\sqrt{2} B_I \lambda}{\xi B_c d} \left[\frac{1}{f^2} - \frac{1}{24} \frac{d^2}{\lambda^2} \right], \quad (5)$$

$$B_I = \mu_0 \langle j_s \rangle \frac{d}{2} + f^2 \frac{d}{2\ell} B_0 = \mu_0 \frac{I_s}{2W} + f^2 \frac{d}{2\ell} B_0, \quad (6)$$

$$0 = \xi^2 k^2 - \frac{\xi k}{6\sqrt{2}} \frac{B_I d}{B_c \lambda} + \left(\frac{1}{24} \frac{B_0^2}{B_c^2} + \frac{1}{160} \frac{B_I^2}{B_c^2} \right) \frac{d^2}{\lambda^2} - 1 + f^2 + \xi k \frac{\sqrt{2}\lambda}{\ell} \frac{B_0}{B_c} - \frac{1}{4} \frac{B_0}{B_c} \frac{B_I d}{B_c \ell}. \quad (7)$$

Apart from the averaging, the above system of equations for k , f , and B_I , in terms of experimentally-defined B_0

and I_s , becomes exact. The nonlinearity and algebraic complexity preclude writing the closed-form analytical solutions of Eqs. (7)-(5). However, from Eq. (7) it is clear that the *magneto-chiral term* $\propto B_0 B_I d/\ell \sim B_0 \langle j_s \rangle d/\ell$ gives the condensate wave function f , and hence the maximal supercurrent j_s^{\max} the condensate can carry, a non-trivial dependence on the mutual orientations of \mathbf{B}_{ext} and \mathbf{j}_s . Furthermore, the strength of the magneto-chiral effect is also driven by the thickness d and the product of the Rashba SOC strength and g-factor, $1/\ell \simeq g\alpha_R$, recall Eq. (2).

To derive some analytical results, we systematically keep only linear and quadratic terms in the small parameters d/λ and d/ℓ , as well as linear terms in B_I/B_c . For thin films, B_0 can be up to parallel-critical-field $B_{c\parallel} = 2\sqrt{6}B_c\lambda/d \gg B_c$, and therefore, we do not employ any restriction on B_0/B_c . While these approximations simplify the system of algebraic equations, their closed solutions are still too cumbersome to be written explicitly. One can show that by keeping B_0 fixed and varying $\langle j_s \rangle$ compared to 0. The physical solutions possess real-valued k and positive-valued f^2 . However, there exists positive and negative maximal supercurrent densities $j_{s>}^{\max} > 0$ and $j_{s<}^{\max} < 0$ that when overcome by $\langle j_s \rangle$, the physical solutions no longer exist. At these points the system undergoes the first-order phase transition and jumps from the superconducting into the normal phase. While the expressions for $j_{s>}^{\max}$ and $j_{s<}^{\max}$ remain complex, the SDE difference $\Delta j_s^{\text{SDE}} = j_{s>}^{\max} - |j_{s<}^{\max}|$, within the considered approximations, has a compact form [57]

$$\Delta j_s^{\text{SDE}} = \frac{B_c d^2}{54\mu_0\lambda} \left(\frac{B_0 \lambda}{B_c \ell} \right) \left[2 + \left(\frac{B_0 \lambda}{B_c \ell} \right)^2 \right]^2. \quad (8)$$

We compare the accuracy of this approximate SDE result in Eq. (8) with the full numerical solution of Eqs. (5)-(7), without any approximations, in Fig. 1(b). The deviations at higher fields stem from the employed approximation which neglects some higher-order terms.

We observe that in quasi-2D films $\Delta j_s^{\text{SDE}} \propto d^2$, i.e., the SDE effect based on the lowest-order LI vanishes as $d \rightarrow 0$, as expected from the assumption that LI could be removed by a gauge transformation. An analog of the higher-order LI that works for a pure 2D system was proposed in Ref. [36]. Furthermore, the derivative of Δj_s^{SDE} with respect to the external field is

$$\left. \frac{d}{dB_0} \Delta j_s^{\text{SDE}} \right|_{B_0=0} = \frac{2}{27\mu_0} \frac{1}{\ell} \frac{d^2}{\lambda^2} = \frac{1}{18\mu_0} \frac{g\alpha_R}{E_F} \frac{d^2}{\lambda^4}, \quad (9)$$

which allows one to extract $1/\ell = (3/4)g\alpha_R/(E_F\lambda^2)$, and hence the ratio of the Rashba SOC and Fermi energy. Thus the SOC characteristics of quasi-2D films can be probed by the SDE in the superconducting phase.

SDE and CPR in SNS Josephson junctions:

As the second example, we consider a long ballistic SNS JJ consisting of noncentrosymmetric S and N elements and look for a solution $\tilde{\psi}$ of Eqs. (3) in the $2L$ -long N-region; see the inset in Fig. 2. The junction is placed in

an in-plane field $\mathbf{B}_{ext} = B_0 \hat{y}$ and carries a steady supercurrent I_s ; for the induced field \mathbf{B}_{ind} and the vector potential \mathbf{A} we employ the same ansatz and Coulomb gauge as before. Requiring the continuity of the condensate wave functions, we match $\tilde{\psi}(x)$ at $x = \pm L$ with $\psi(x) = f e^{ikx \pm i\varphi/2}$, in the sufficiently long and wide identical left and right superconductors, S. The total phase difference between their ends is $-\varphi + 2kL$, see the inset in Fig. 2. The external phase φ can be controlled, e.g., by a flux loop. To distinguish the parameters and quantities in the S and N regions, we use the tilde symbols for those associated with N, for example, $\tilde{a} > 0$, while $a < 0$.

Following a similar procedure for a thin film, we transversely average GL Eqs. (3) and (4) as well as linearize them (ignoring the cubic term in $\tilde{\psi}$), since the JJ is long and the proximity-induced $\tilde{\psi}$ is suppressed. The resulting equation for $\tilde{\psi}$, including the diamagnetic terms, is

$$0 = \frac{d^2 \tilde{\psi}}{dx^2} - 2i \underbrace{\frac{1}{\sqrt{2\xi}} \left[\frac{1}{12} \frac{\tilde{d}}{\tilde{\lambda}} \frac{\tilde{B}_I}{\tilde{B}_c} - \frac{\tilde{\lambda} B_0}{\tilde{\ell} \tilde{B}_c} \right]}_{\varepsilon} \frac{d\tilde{\psi}}{dx} - \underbrace{\frac{1}{\xi^2} \left[1 - \frac{\tilde{d}}{4\tilde{\ell}} \frac{B_0 \tilde{B}_I}{\tilde{B}_c^2} + \frac{\tilde{d}^2}{\tilde{\lambda}^2} \left(\frac{B_0^2}{24\tilde{B}_c^2} + \frac{\tilde{B}_I^2}{160\tilde{B}_c^2} \right) \right]}_{\tilde{\alpha} > 0} \tilde{\psi}, \quad (10)$$

where due to the linearization, $\tilde{B}_I = \mu_0 \langle \tilde{j}_s \rangle \tilde{d}/2$. The solution of the above equation is a superposition of $e^{i\tilde{\varepsilon}x + \tilde{q}x}$ and $e^{i\tilde{\varepsilon}x - \tilde{q}x}$, where, $\tilde{q} = \sqrt{\tilde{\alpha} - \tilde{\varepsilon}^2}$. Matching it with the wave functions in left and right S, one gets $\tilde{\psi}(x)$ and, according to Eq. (4), the supercurrent density

$$\tilde{j}_s(\varphi) = \sqrt{8\tilde{q}} f^2 \frac{m}{\tilde{m}} \frac{B_c}{\mu_0} \frac{\xi}{\lambda} \sin[(\varphi - 2kL) + 2\tilde{\varepsilon}L] e^{-2\tilde{q}L}, \quad (11)$$

where f , k , ξ , λ , and B_c correspond to the two S regions, while the ratio m/\tilde{m} accounts for different effective masses (density of states) in the S and N.

Our expression Eq. (11) is a generalization of the result for anomalous phase shift $\phi_0 = -4L\tilde{K}\tilde{m}B_0/\hbar$ from Ref. [58] for the noncentrosymmetric SNS junction, but with (i) considering the LI only inside the N region and (ii) a calculation limited by including only B_0/\tilde{B}_c term, ignoring its higher powers and also \tilde{B}_I/\tilde{B}_c terms. Unlike this result, which yields a simple ϕ_0 -shift in the harmonic CPR and no SDE [20], our Eq. (11), as we discussed below, reveals several key differences in $\tilde{j}_s(\varphi)$, including robust SDE and strong anharmonicity, characteristic also for JJs revealing topological superconductivity [21]. All magneto-chiral terms $\propto 1/\tilde{\ell}$ and those induced by $\tilde{j}_s(\varphi) \sim \tilde{B}_I$ itself, give rise to the dynamically-generated CPR stemming from the self-consistent problem, $\tilde{j}_s(\varphi) = \mathbb{F}[\tilde{j}_s(\varphi)]$: **(1)** Having a supercurrent I_s passing through the SNS junction, we calculate the supercurrent densities $\langle j_s \rangle = I_s/(Wd)$ and $\langle \tilde{j}_s \rangle = I_s/(W\tilde{d})$ in the S and N regions; **(2)** Obtained $\langle j_s \rangle$ in the S region

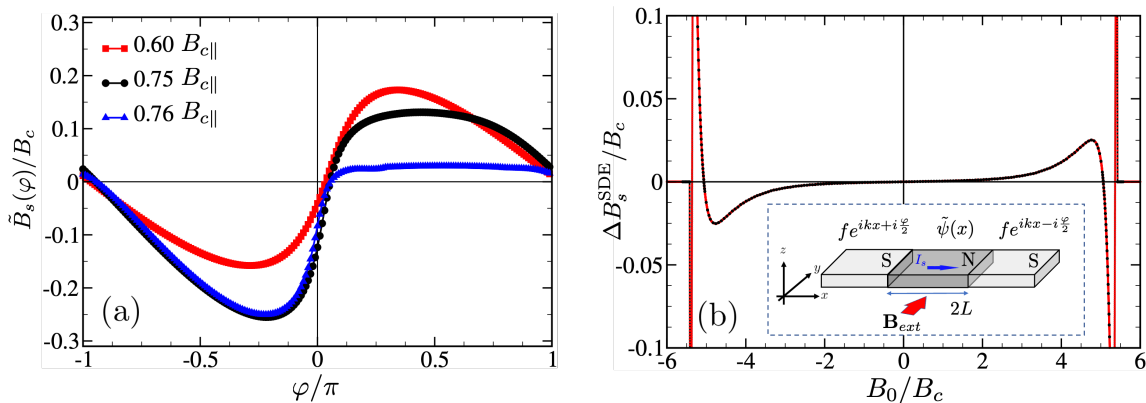


FIG. 2. CPR and SDE for a long noncentrosymmetric SNS JJ with the same parameters in the N and S regions, i.e., $\xi = \tilde{\xi}$, $\lambda = \tilde{\lambda}$, $\ell = \tilde{\ell}$, $d = \tilde{d}$, and $m = \tilde{m}$: (a) Distorted CPRs, for different external fields: 0.6 (red), 0.75 (black), and 0.76 (blue) multiples of parallel-critical-field, $B_{c||}$, shown $\tilde{B}_s(\varphi) = \mu_0 \tilde{j}_s(\varphi) \tilde{d}/2$, normalized to $B_c = \tilde{B}_c$, as a function of φ/π . (b) SDE versus the in-plane field B_0 , normalized to B_c . The supercurrent difference $\Delta \tilde{j}_s^{\text{SDE}}$ is converted to the corresponding field difference $\Delta \tilde{B}_s^{\text{SDE}} = \mu_0 \Delta \tilde{j}_s^{\text{SDE}} \tilde{d}/2$ and is plotted in units of B_c . The black symbols: computed data points, red curve: an interpolation line. Inset: JJ geometry with the phase difference $-\varphi + 2kL$. Here, $\xi/\lambda = 1.3$, $\ell/\lambda = 3$, $d/\lambda = 0.7$, and $L/\lambda = 1.95$.

defines, for a given external field B_0 , the dimensionless wave functions, f , wave vector, k , and induced field, B_I , see Eqs.(5)–(7); (3) Knowing $\langle \tilde{j}_s \rangle$ specifies \tilde{B}_I , $\tilde{\varepsilon}$, and \tilde{q} , which, along with the values of f and k , specify the CPR $\tilde{j}_s(\varphi)$ according to Eq. (11); (4) The phase difference φ_{I_s} corresponding to the given supercurrent I_s should be chosen such that $\tilde{j}_s(\varphi_{I_s}) = I_s/(\tilde{W}\tilde{d}) = \langle \tilde{j}_s \rangle$.

The results of the above self-consistent procedure are displayed in Fig. 2(a), which shows the anharmonic CPR for the fully symmetric SNS junction with $L/\lambda = 1.95$, $d/\lambda = 0.7$, and several in-plane fields. The pronounced harmonic distortion of the CPR when evolving the phase φ gives, for different external fields, different magnitudes of positive, $\tilde{j}_{s>}^{\text{max}}$, and negative, $\tilde{j}_{s<}^{\text{max}}$, critical currents, i.e., the JJ SDE. We plot the corresponding SDE difference $\Delta \tilde{j}_s^{\text{SDE}} = \tilde{j}_{s>}^{\text{max}} - |\tilde{j}_{s<}^{\text{max}}|$ with the in-plane B_0 in Fig. 2(b). For positive B_0 , with its increase, $\Delta \tilde{j}_s^{\text{SDE}}$ gradually grows, first linearly, and then with admixed cubic and quintic dependence on B_0 . However, at a certain field range ($B_0/B_c \sim 5$), the SDE starts to saturate, then decreasing, crossing to negative values and again upturning and returning to zero. Numerical data in the sign-changed transition region are showing a certain numerical instability, e.g. CPR does not exist for all phases or becomes multi-valued, therefore we plot the reliable data points by black symbols, and their interpolation, including the unstable region, with red line.

Conclusions: Our theoretical framework offers a transparent and unified approach to analyze the SDE in different structures and use it to probe the SOC in quasi-2D systems. Surprisingly, a self-consistent solution to simple algebraic equations already provides an important tool to examine the magnetochiral properties of JJs, including the anomalous phase shift, anharmonic CPR, and the sign reversal of the SDE at high magnetic

fields. These signatures are also important in the studies of topological superconductivity [18, 21], while the spin-triplet proximity-induced superconductivity accompanying the SDE in noncentrosymmetric systems is directly relevant for superconducting spintronics [20].

While we have focused on a commonly assumed SOC linear in the wave vector, our approach could be also generalized to consider an anisotropic LI [48] inherent to JJs with cubic SOC [59, 60] and look also for its a non-linear and even multi-component order-parameter generalizations [46, 61]. The resulting proximity-induced f -wave superconductivity [59], along with including the nonlinear Meissner effect [62–66] provides unexplored directions for SDE studies and their implications for unconventional superconductivity. With the AC applied magnetic field, the generation of higher harmonics [59, 67] and their anisotropy could be used to measure the resulting non-linear [63, 66] and magnetochiral contributions.

Acknowledgements: We thank C. Strunk, N. Paradiso, J. Fabian, D. Agterberg, L. Rokhinson, A. Buzdin, M. Milošević, and A. Vagov for useful discussions. D.K. acknowledges a partial support from the IMPULZ project IM-2021-26—SUPERSPIN funded by the Slovak Academy of Sciences, VEGA Grant No. 2/0156/22—QuaSiModo, and from the COST Action CA21144—SUPERQUMAP. Work in Regensburg was partly supported by Deutsche Forschungsgemeinschaft (DFG, German Research Foundation) within Project-ID 314695032—SFB 1277 (projects A07 and B07) and Project-ID 454646522—“Spin and magnetic properties of superconducting tunnel junctions”. I.Ž. was supported by the U.S. ONR through Grants No. N000141712793 and MURI No. N000142212764, and NSF Grant No. ECCS-2130845.

- [1] C. Coulais, D. Sounas, and A. Alù, Static non-reciprocity in mechanical metamaterials, *Nature* **542**, 461 (2017).
- [2] I. V. Shadrivov, V. A. Fedotov, D. A. Powell, Y. S. Kivshar, and N. I. Zheludev, Electromagnetic wave analogue of an electronic diode, *New J. Phys.* **13**, 033025 (2011).
- [3] C. Caloz, A. Alù, S. Tretyakov, D. Sounas, K. Achouri, and Z.-L. Deck-Léger, Electromagnetic Nonreciprocity, *Phys. Rev. Appl.* **10**, 047001 (2018).
- [4] M. Faraday, On the magnetization of light and the illumination of magnetic lines of force, *Philos. Trans. R. Soc.* **136**, 1 (1846).
- [5] J. Kerr, On rotation of the plane of polarization by reflection from the pole of a magnet, *Philos. Mag.* **3**, 321 (1877).
- [6] W. Shockley and E. M. Field, Electrons and Holes in Semiconductors, *Phys. Today* **5**, 18 (1952).
- [7] I. Žutić, J. Fabian, and S. Das Sarma, Spintronics: Fundamentals and applications, *Rev. Mod. Phys.* **76**, 323 (2004).
- [8] R. Waser, ed., *Nanoelectronics and information technology*, 3rd ed. (Wiley-VCH Verlag, Weinheim, Germany, 2012).
- [9] E. Y. Tsymbal and I. Žutić, *Spintronics Handbook: Spin Transport and Magnetism, Second Edition*, edited by E. Y. Tsymbal and I. Žutić (CRC Press, 2019).
- [10] R. Wakatsuki, Y. Saito, S. Hoshino, Y. M. Itahashi, T. Ideue, M. Ezawa, Y. Iwasa, and N. Nagaosa, Nonreciprocal charge transport in noncentrosymmetric superconductors, *Sci. Adv.* **3**, e1602390 (2017).
- [11] Y. M. Itahashi, T. Ideue, Y. Saito, S. Shimizu, T. Ouchi, T. Nojima, and Y. Iwasa, Nonreciprocal transport in gate-induced polar superconductor SrTiO₃, *Sci. Adv.* **6**, eaay9120 (2020).
- [12] F. Ando, Y. Miyasaka, T. Li, J. Ishizuka, T. Arakawa, Y. Shiota, T. Moriyama, Y. Yanase, and T. Ono, Observation of superconducting diode effect, *Nature* **584**, 373 (2020).
- [13] C. Baumgartner, L. Fuchs, A. Costa, S. Reinhardt, S. Gronin, G. C. Gardner, T. Lindemann, M. J. Manfra, P. E. Faria Junior, D. Kochan, J. Fabian, N. Paradiso, and C. Strunk, Supercurrent rectification and magnetochiral effects in symmetric Josephson junctions, *Nat. Nanotechnol.* **17**, 39 (2022).
- [14] H. Wu, Y. Wang, Y. Xu, P. K. Sivakumar, C. Pasco, U. Filippozzi, S. S. P. Parkin, Y.-J. Zeng, T. McQueen, and M. N. Ali, The field-free Josephson diode in a van der Waals heterostructure, *Nature* **604**, 653 (2022).
- [15] K.-R. Jeon, J.-K. Kim, J. Yoon, J.-C. Jeon, H. Han, A. Cottet, T. Kontos, and S. S. P. Parkin, Zero-field polarity-reversible Josephson supercurrent diodes enabled by a proximity-magnetized Pt barrier, *Nat. Mater.* **21**, 1008 (2022).
- [16] B. Pal, A. Chakraborty, P. K. Sivakumar, M. Davydova, A. K. Gopi, A. K. Pandeya, J. A. Krieger, Y. Zhang, M. Date, S. Ju, N. Yuan, N. B. M. Schröter, L. Fu, and S. S. P. Parkin, Josephson diode effect from Cooper pair momentum in a topological semimetal, *Nat. Phys.* **18**, 1228 (2022).
- [17] A. Costa, C. Baumgartner, S. Reinhardt, J. Berger, S. Gronin, G. C. Gardner, T. Lindemann, M. J. Manfra, D. Kochan, J. Fabian, N. Paradiso, and C. Strunk, Sign reversal of the AC and DC supercurrent diode effect and 0- π -like transitions in ballistic Josephson junctions (2022), [arXiv:2212.13460](https://arxiv.org/abs/2212.13460).
- [18] N. Lotfizadeh, B. Pekerten, P. Yu, W. Strickland, A. Matos-Abiague, and J. Shabani, Superconducting Diode Effect Sign Change in Epitaxial Al-InAs Josephson Junctions (2023), [arXiv:2303.01902](https://arxiv.org/abs/2303.01902).
- [19] M. Nadeem, M. S. Fuhrer, and X. Wang, Superconducting Diode Effect – Fundamental Concepts, Material Aspects, and Device Prospects (2023), [arXiv:2301.13564](https://arxiv.org/abs/2301.13564).
- [20] M. Amundsen, J. Linder, J. W. A. Robinson, I. Žutić, and N. Banerjee, Colloquium: Spin-orbit effects in superconducting hybrid structures (2022), [arXiv:2210.03549](https://arxiv.org/abs/2210.03549).
- [21] M. C. Dartiailh, W. Mayer, J. Yuan, K. S. Wickramasinghe, A. Matos-Abiague, I. Žutić, and J. Shabani, Phase Signature of Topological Transition in Josephson Junctions, *Phys. Rev. Lett.* **126**, 036802 (2021).
- [22] J. Hu, C. Wu, and X. Dai, Proposed Design of a Josephson Diode, *Phys. Rev. Lett.* **99**, 067004 (2007).
- [23] J. Diez-Merida, A. Diez-Carlon, S. Y. Yang, Y. M. Xie, X. J. Gao, K. Watanabe, T. Taniguchi, X. Lu, K. T. Law, and D. K. Efetov, Magnetic Josephson Junctions and Superconducting Diodes in Magic Angle Twisted Bilayer Graphene (2021), [arXiv:2110.01067](https://arxiv.org/abs/2110.01067).
- [24] C. Baumgartner, L. Fuchs, A. Costa, J. Picó-Cortés, S. Reinhardt, S. Gronin, G. C. Gardner, T. Lindemann, M. J. Manfra, P. E. F. Junior, D. Kochan, J. Fabian, N. Paradiso, and C. Strunk, Effect of Rashba and Dresselhaus spin-orbit coupling on supercurrent rectification and magnetochiral anisotropy of ballistic Josephson junctions, *J. Phys.: Condens. Matter* **34**, 154005 (2022).
- [25] L. Bauriedl, C. Bäuml, L. Fuchs, C. Baumgartner, N. Paulik, J. M. Bauer, K.-Q. Lin, J. M. Lupton, T. Taniguchi, K. Watanabe, C. Strunk, and N. Paradiso, Supercurrent diode effect and magnetochiral anisotropy in few-layer NbSe₂, *Nat. Commun.* **13**, 4266 (2022).
- [26] B. Turini, S. Salimian, M. Carrega, A. Iorio, E. Strambini, F. Giazotto, V. Zannier, L. Sorba, and S. Heun, Josephson Diode Effect in High-Mobility InSb Nanoflags, *Nano Lett.* **22**, 8502 (2022).
- [27] J.-X. Lin, P. Siriviboon, H. D. Scammell, S. Liu, D. Rhodes, K. Watanabe, T. Taniguchi, J. Hone, M. S. Scheurer, and J. I. A. Li, Zero-field superconducting diode effect in small-twist-angle trilayer graphene, *Nat. Phys.* **18**, 1221 (2022).
- [28] V. M. Edelstein, Characteristics of the Cooper pairing in two-dimensional noncentrosymmetric electron systems, *Sov. Phys. - JETP* **68**, 1244 (1989).
- [29] V. M. Edelstein, The Ginzburg - Landau equation for superconductors of polar symmetry, *J. Phys.: Condens. Matter* **8**, 339 (1996).
- [30] O. Dimitrova and M. V. Feigel'man, Theory of a two-dimensional superconductor with broken inversion symmetry, *Phys. Rev. B* **76**, 014522 (2007).
- [31] R. Grein, M. Eschrig, G. Metalidis, and G. Schön, Spin-Dependent Cooper Pair Phase and Pure Spin Supercurrents in Strongly Polarized Ferromagnets, *Phys. Rev. Lett.* **102**, 227005 (2009).
- [32] V. P. Mineev and M. Sigrist, Basic Theory of Superconductivity in Metals Without Inversion Center, in *Non-*

- Centrosymmetric Superconductors*, edited by E. Bauer and M. Sigrist (Springer Berlin Heidelberg, 2012) pp. 129–154.
- [33] A. Daido, Y. Ikeda, and Y. Yanase, Intrinsic Superconducting Diode Effect, *Phys. Rev. Lett.* **128**, 037001 (2022).
- [34] N. F. Q. Yuan and L. Fu, Supercurrent diode effect and finite-momentum superconductors, *PNAS* **119**, e2119548119 (2022).
- [35] M. Smith, A. V. Andreev, and B. Z. Spivak, Giant magnetoconductivity in noncentrosymmetric superconductors, *Phys. Rev. B* **104**, L220504 (2021).
- [36] J. J. He, Y. Tanaka, and N. Nagaosa, A phenomenological theory of superconductor diodes, *New J. Phys.* **24**, 053014 (2022).
- [37] H. D. Scammell, J. I. A. Li, and M. S. Scheurer, Theory of zero-field superconducting diode effect in twisted trilayer graphene, *2D Mater.* **9**, 025027 (2022).
- [38] S. Ilić and F. S. Bergeret, Theory of the Supercurrent Diode Effect in Rashba Superconductors with Arbitrary Disorder, *Phys. Rev. Lett.* **128**, 177001 (2022).
- [39] M. Davydova, S. Prembabu, and L. Fu, Universal Josephson diode effect, *Sci. Adv.* **8**, eabo0309 (2022).
- [40] T. de Picoli, Z. Blood, Y. Lyanda-Geller, and J. I. Väyrynen, Superconducting diode effect in quasi-one-dimensional systems (2023), [arXiv:2302.04277](https://arxiv.org/abs/2302.04277).
- [41] L. Fuchs, D. Kochan, J. Schmidt, N. Hüttner, C. Baumgartner, S. Reinhardt, S. Gronin, G. C. Gardner, T. Lindemann, M. J. Manfra, C. Strunk, and N. Paradiso, Anisotropic Vortex Squeezing in Synthetic Rashba Superconductors: A Manifestation of Lifshitz Invariants, *Phys. Rev. X* **12**, 041020 (2022).
- [42] Y. Hou, F. Nichele, H. Chi, A. Lodesani, Y. Wu, M. F. Ritter, D. Z. Haxell, M. Davydova, S. Ilić, O. Glezakou-Elbert, A. Varambally, F. S. Bergeret, A. Kamra, L. Fu, P. A. Lee, and J. S. Moodera, Ubiquitous Superconducting Diode Effect in Superconductor Thin Films (2023), [arXiv:2205.09276](https://arxiv.org/abs/2205.09276).
- [43] A. Banerjee, M. Geier, M. A. Rahman, C. Thomas, T. Wang, M. J. Manfra, K. Flensberg, and C. M. Marcus, Phase Asymmetry of Andreev Spectra From Cooper-Pair Momentum (2023), [arXiv:2301.01881](https://arxiv.org/abs/2301.01881).
- [44] A. Sundaresh, J. I. Väyrynen, Y. Lyanda-Geller, and L. P. Rokhinson, Diamagnetic mechanism of critical current non-reciprocity in multilayered superconductors (2023), [arXiv:2207.03633](https://arxiv.org/abs/2207.03633).
- [45] D. Suri, A. Kamra, T. N. G. Meier, M. Kronseder, W. Belzig, C. H. Back, and C. Strunk, Non-reciprocity of vortex-limited critical current in conventional superconducting micro-bridges, *Appl. Phys. Lett.* **121**, 102601 (2022).
- [46] V. Mineev and K. Samokhin, Helical phases in superconductors, *Soviet Journal of Experimental and Theoretical Physics* **78**, 401 (1994).
- [47] V. M. Edelstein, Magnetoelectric Effect in Polar Superconductors, *Phys. Rev. Lett.* **75**, 2004 (1995).
- [48] K. V. Samokhin, Magnetic properties of superconductors with strong spin-orbit coupling, *Phys. Rev. B* **70**, 104521 (2004).
- [49] V. P. Mineev and K. V. Samokhin, Nonuniform states in noncentrosymmetric superconductors: Derivation of Lifshitz invariants from microscopic theory, *Phys. Rev. B* **78**, 144503 (2008).
- [50] D. F. Agterberg, Magnetoelectric Effects, Helical Phases, and FFLO Phases, in *Non-Centrosymmetric Superconductors*, edited by E. Bauer and M. Sigrist (Springer Berlin Heidelberg, 2012) pp. 155–170.
- [51] E. M. Lifshitz, On the theory of the second order phase-transitions I., *JETP* **11**, 255 (1941).
- [52] E. M. Lifshitz, On the theory of the second order phase-transitions II., *JETP* **11**, 269 (1941).
- [53] The coupling constant \mathcal{K} is also temperature, T , dependent, the full expression is $\mathcal{K} = 3 \frac{\alpha_R}{\hbar} \frac{g \mu_B}{v_F p_F} f_3 \left(\frac{\alpha_R p_F}{\hbar \pi k_B T} \right)$, where $f_3(x) \simeq 0.475 \int_0^\pi dt \sum_{n=0}^{\infty} \frac{\sin t (x \sin t)^2}{(2n+1)^3 [(2n+1)^2 + (x \sin t)^2]}$. Approximation in the main text holds for low T .
- [54] At the interface to vacuum, from the variation of F , one obtains the boundary condition $0 = (\hat{\nu}_{\text{out}} \cdot \mathbf{D}_{\mathcal{K}}) \psi \Big|_{\text{interface}}$, where $\hat{\nu}_{\text{out}}$ is the unit normal vector to the interface pointing into vacuum. In this work, all condensate wavefunctions satisfy the above boundary conditions.
- [55] M. Smidman, M. B. Salamon, H. Q. Yuan, and D. F. Agterberg, Superconductivity and spin-orbit coupling in non-centrosymmetric materials: A review, *Rep. Prog. Phys.* **80**, 36501 (2017).
- [56] V. Schmidt, *The Physics of Superconductors: Introduction to Fundamentals and Applications*, edited by P. Müller and A. Ustinov (Springer, 1997).
- [57] The corresponding SDE efficiency $\eta_s^{\text{SDE}} = (j_{s>}^{max} - |j_{s<}^{max}|) / (j_{s>}^{max} + |j_{s<}^{max}|)$ within the same level of approximation equals $\eta_s^{\text{SDE}} \simeq \frac{\sqrt{3}}{36} \frac{d^2}{\lambda^2} \left(\frac{B_0}{B_{cm}} \frac{\lambda}{\ell} \right) \left[2 + \left(\frac{B_0}{B_{cm}} \frac{\lambda}{\ell} \right)^2 \right]^{\frac{1}{2}}$.
- [58] A. Buzdin, Direct Coupling Between Magnetism and Superconducting Current in the Josephson φ_0 Junction, *Phys. Rev. Lett.* **101**, 107005 (2008).
- [59] M. Alidoust, C. Shen, and I. Žutić, Cubic spin-orbit coupling and anomalous Josephson effect in planar junctions, *Phys. Rev. B* **103**, L060503 (2021).
- [60] M. Luethi, K. Laubscher, S. Bosco, D. Loss, and J. Klinovaja, Planar Josephson junctions in germanium: Effect of cubic spin-orbit interaction, *Phys. Rev. B* **107**, 035435 (2023).
- [61] K. V. Samokhin, Helical states and solitons in noncentrosymmetric superconductors, *Phys. Rev. B* **89**, 094503 (2014).
- [62] D. Xu, S. K. Yip, and J. A. Sauls, Nonlinear Meissner effect in unconventional superconductors, *Phys. Rev. B* **51**, 16233 (1995).
- [63] A. Bhattacharya, I. Zutic, O. T. Valls, A. M. Goldman, U. Welp, and B. Veal, Angular Dependence of the Nonlinear Transverse Magnetic Moment of $\text{YBa}_2\text{Cu}_3\text{O}_{6.95}$ in the Meissner State, *Phys. Rev. Lett.* **82**, 3132 (1999).
- [64] A. P. Zhuravel, B. G. Ghamsari, C. Kurter, P. Jung, S. Remillard, J. Abrahams, A. V. Lukashenko, A. V. Ustinov, and S. M. Anlage, Imaging the Anisotropic Nonlinear Meissner Effect in Nodal $\text{YBa}_2\text{Cu}_3\text{O}_{7-\delta}$ Thin-Film Superconductors, *Phys. Rev. Lett.* **110**, 087002 (2013).
- [65] I. Žutić and O. T. Valls, Superconducting-gap-node spectroscopy using nonlinear electrodynamics, *Phys. Rev. B* **56**, 11279 (1997).
- [66] I. Žutić and O. T. Valls, Low-frequency nonlinear magnetic response of an unconventional superconductor, *Phys. Rev. B* **58**, 8738 (1998).
- [67] Y. Fukaya, Y. Tanaka, P. Gentile, K. Yada, and M. Cuoco, Anomalous Josephson Coupling and

High-Harmonics in Non-Centrosymmetric Superconductors with *S*-wave Spin-Triplet Pairing (2022), [arXiv:2204.14083](https://arxiv.org/abs/2204.14083).